ADVANCED FUNCTIONAL MATERIALS
www.afm-journal.de

Stable Light-Emitting Electrochemical Cells Using Hyperbranched Polymer Electrolyte

*Lorenzo Mardegan, Chris Dreessen, Michele Sessolo, Daniel Tordera, and Henk J. Bolink**

The choice of an adequate electrolyte is a fundamental aspect in polymer light-emitting electrochemical cells (PLECs) as it provides the in situ electrochemical doping and influences the performance of these devices. In this study, a hyperbranched polymer (Hybrane DEO750 8500) blended with a Li salt is used as a novel electrolyte in state-of-the-art Super Yellow (a polyphenylenevinylene) based LECs. Due to the desirable properties of the hyperbranched polymer and the homogeneous and smooth films that it forms with the emitting polymer, PLEC with excellent electroluminescent properties are obtained using a pulsed current bias scheme. The devices are very stable, with lifetimes in excess of 2000 h with initial luminance values above 450 cd m^{-2}, a peak efficiency of 12.6 lm W^{-1}, and sub-minute turn-on times. The stability of the devices is also studied by measuring the photoluminescence (PL) of the semiconductor during electroluminescent operation. The findings suggest that it is possible to observe the quenching of the PL in vertically stacked devices due to the advancement of the doped fronts in the film and an immediate PL recovery when the bias is removed.

1. Introduction

Organic light-emitting diodes (OLEDs) are currently one of the preferred technologies for display applications in consumer electronics such as smartphones and TV screens. Their high image quality (e.g., contrast ratio and viewing angle), good power efficiency (PE), and fast response time, combined with the possibility to use lightweight and flexible plastic substrates make them an attractive solution for high-end products.[1] However, their fabrication costs limit their entry into the general lighting market where low-cost is a key parameter to compete with the existing lighting technologies. OLEDs are devices based on multilayer architectures that require a rigorous encapsulation to prevent degradation of the air-sensitive electrodes, and their processing consists of a large number of steps, most of which have to be done by evaporation techniques. In contrast to OLEDs, light-emitting electrochemical cells (LECs) have a much simpler layout consisting of an intimate blend of an electrolyte, that provides mobile ions, and a semiconducting electroluminescent material as the active layer, processed via solution techniques and sandwiched between two air-stable electrodes. LECs unique operation mechanism is based on the presence of both electronic and ionic conductors.[2] Upon the application of a bias the ions redistribute within the active layer allowing efficient electronic charge carrier injection at the electrodes, transport, and recombination.[2–7] Hence, the electrolyte plays a key role in determining the overall performance of LECs. The electroluminescent material can either be a conjugated polymer (CP),[2,8,9] a conjugated small molecule (SM),[10–14] or a transition metal complex (iTMC).[15–18] In LECs where the light-emitting material is a conjugated polymer (PLECs) one way to add ionic conductors is by using a polymer electrolyte which consists of a salt and a coordinating polymer that dissolves and coordinates the ions thanks to its electron donor centers.[19] LECs based on fluorescent CPs are attractive for their ease of processability, lower costs, and great compatibility with flexible substrates. However, CPs are limited as they can only harvest singlets which make them intrinsically less efficient than phosphorescent iTMCs that can harvest both singlets and triplets.[20] Improving the performance, in particular the stability, of LECs is challenging as the mechanism responsible for facile charge injection with air-stable electrodes also leads to an increased quenching of excited states over time, and thus to a decrease of the luminance levels.[4,21] Charge injection is facilitated by the build-up of ions at the electrode interfaces through an increase in the effective electric field. Upon electron injection at the cathode the uncompensated cations redistribute and stabilize the reduced segments on the CP chain. At the anode, the same occurs by uncompensated anions and oxidized segments on the CP. These interactions between electronic and ionic charges are generally referred to as doping, as it increases the effective charge density in the system, and as such increases the conductivity. However, as there is no physical separation between the area of exciton generation and the doped regions, part of the excitons are quenched due to the interaction with

L. Mardegan, C. Dreessen, M. Sessolo, D. Tordera, H. J. Bolink
Instituto de Ciencia Molecular (ICMol)
Universidad de Valencia
C/Catedratico J. Beltran 2 Paterna, Valencia 46980, Spain
E-mail: henk.bolink@uv.es

The ORCID identification number(s) for the author(s) of this article can be found under https://doi.org/10.1002/adfm.202104249.

DOI: 10.1002/adfm.202104249

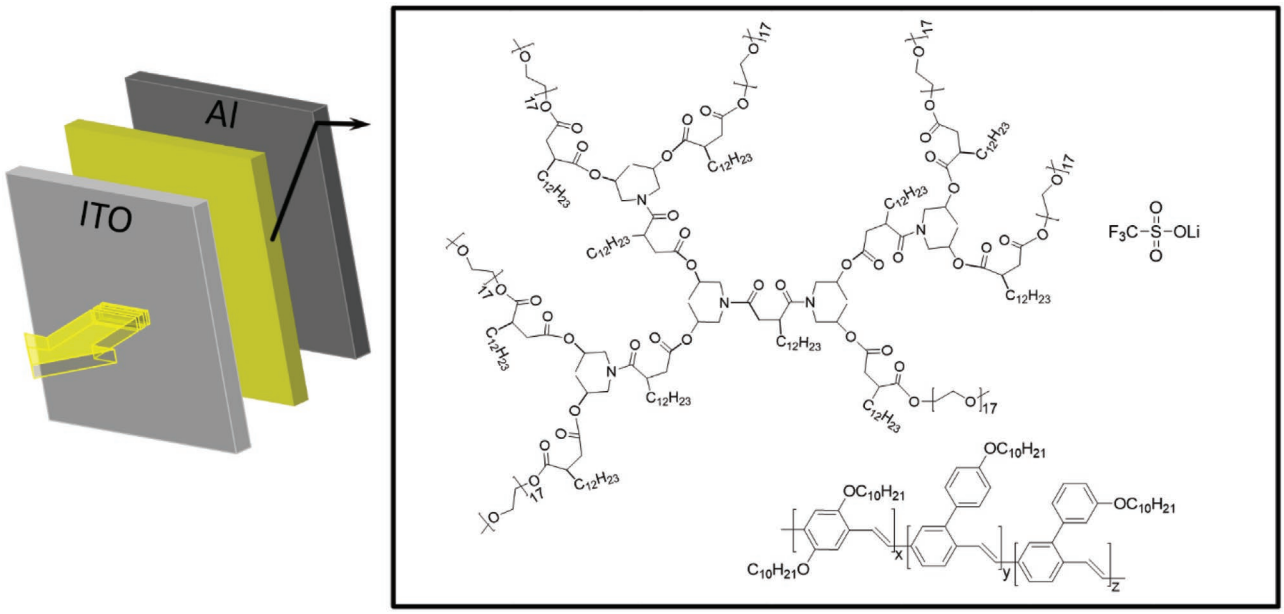

Figure 1. Scheme of the final device architecture and chemical structure of the components of the active layer: the ion dissolving hyperbranched polymer (Hybrane), the lithium trifluoromethanesulfonate salt, and the semiconducting polymer SY.

the radical cations and anions present in the doped regions.[6] Hence, to improve the performance of LECs one must be able to prevent as much as possible the interaction between the doped regions and the active intrinsic region where the excitons are generated. As doping leads to quenching of excitons, photoluminescence (PL) has been used in the past to probe the growth of the doped zones. This is difficult to do in operating devices, as it is not trivial to distinguish between electrically and photo-excited states. Recently, promising results have been attained on devices using Super Yellow (SY), a PPV-based CP, as active material and branched polytrimethylene carbonate (PTMC) electrolytes derivatives showing long operational lifetimes of 138 h at >300 cd m^{-2} and a peak PE of 9.8 lm W^{-1} at a constant current density driving bias of 77 A m^{-2}.[22] Previous works including SY and a star-branched trimethylolpropane ethoxylate (TMPE) derivatives as ion transporter showed exceptional lifetimes longer than 1200 h over 100 cd m^{-2} and maximum PEs of 18.1 lm W^{-1}.[23,24] In this work, we develop LECs based on the archetype polyphenylenevinylene (PPV) CP SY and lithium trifluoromethanesulfonate ($LiCF_3SO_3$, LiTf) salt, combined with a novel hyperbranched ion solvating polymer, Hybrane DEO750 8500 (Hy) (**Figure 1**). The devices show an extrapolated t_{50} of 2000 h (at an initial luminance above 480 cd m^{-2}) and peak power efficiencies of 12.6 lm W^{-1} with sub-minute turn-on times. These lifetime values are amongst the highest reported in the literature for fluorescent LECs. In an attempt to understand the effect of the doped zones formation on the stability we employ frequency-modulated PL probing during steady-state electroluminescence (EL) operation under a forward bias. This allows us to probe the evolution of the PL as a function of driving conditions in operating LECs. Our results suggest that this method could be employed to model how the free ions interact with the polymer matrix in the different stages of operation of a LEC.

2. Results and Discussion

Motivated by the recent advancements in the polymer electrolyte design for LECs we decided to introduce a hyperbranched polymer, Hybrane DEO750 8500, as ion-dissolving and transporting media. To successfully act as a host for free mobile ions, a polymer should have the following characteristics: 1) electron-donor groups or atoms able to coordinate cations; 2) high chain mobility and 3) suitable distance between the coordinating centers.[21,25,26] The Hybrane (Figure 1) displays promising structural features for PLECs applications. At room temperature, the Hybrane is a dense liquid and its backbone structure is constituted of ester and amide groups whereas the chains end with ethyleneoxide units that are methoxy-terminated. In previous works, the ability of ester groups to coordinate and transport metal cations in PLECs has been shown.[22,27,28] Furthermore, a recent study showed that the methoxy ($-OCH_3$) terminal groups provide an enhanced mobility of the cations.[29] The anions, on the other hand, are less restricted by the polymeric host as the host is only able to coordinate the cations,[29,30] consequently they can move faster within the medium. As a result, the p-type doping in LECs is generally faster than the n-type doping. To ensure optimal device performance, thin films should consist of a homogeneous blend between the polymer electrolyte and the semiconducting polymer.[31] When an optimum blend is provided one expects the most favorable salt dispersion over the active area and the most advantageous ion exchange between the ion dissolving polymer and the CP. As stated above, the presence of oxygen coordinating groups mainly helps in the solvation and coordination of the cations, however, the presence of long carbon chains ($-C_{12}H_{23}$) supports blending with the non-polar SY. Thus, its structure could result in a suitable option for a variety of semiconducting polymers.

The interaction between the two components has been investigated in the presence and absence of the lithium salt.

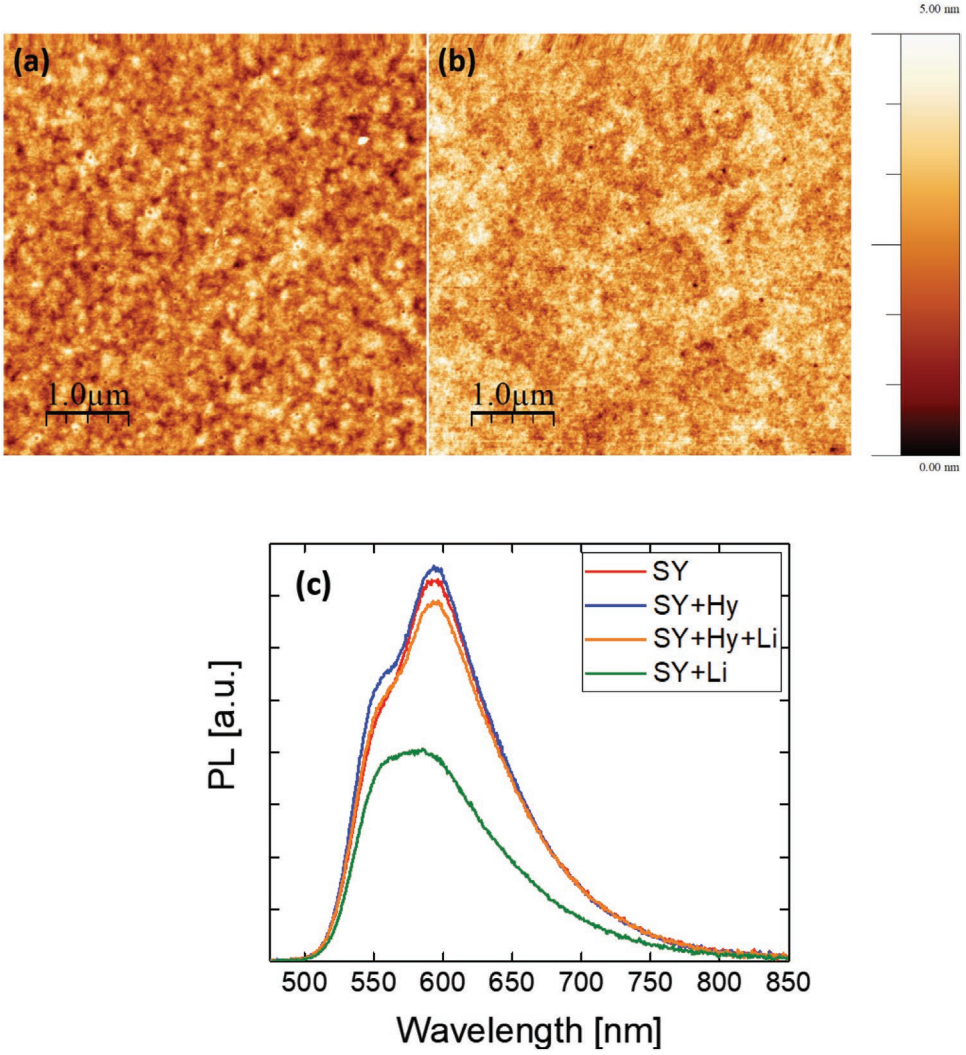

Figure 2. AFM images (5 µm x 5 µm) of a) pristine SY and b) SY + 30 % Hybrane + 9% LiTf coated on glass/ITO substrates. c) PL spectra of SY and SY mixed with Hybrane, Hybrane+LiTf, and LiTf only.

Atomic Force Microscopy (AFM) has been used to establish whether the spin-casted solutions resulted in homogeneous thin films. In **Figure 2**a,b AFM images of pristine SY and blended SY+Hybrane+LiTf samples, deposited on a glass/ITO substrate, are shown, respectively. Details on the preparation of the samples are given in the Experimental Section. The AFM images reveal that both the pristine and blended films are very flat with an average roughness of 0.50 nm and an average height of 2.42 nm for SY (Figure 2a) and 0.43 and 2.97 nm for SY+ Hybrane+LiTf (1:0.3:0.09 mass ratio, Figure 2b). The measured values are in line with recent literature data regarding pristine SY and SY+polymer electrolyte films.[22,32] As a result, both the pristine SY and the blend show very similar surface features indicating that the mixed-polymer matrix appears in an amorphous state and that there is no sign of undesirable phase separation.

Subsequently, we determined the photoluminescence quantum yield (PLQY) of samples consisting of SY with and without Hybrane and the LiTf salt, deposited on a quartz substrate from a cyclohexanone solution. The maximum PLQYs obtained are 75%, 78%, 73%, and 45% for the SY, SY+ Hybrane, SY+Hybrane+LiTf, and SY+LiTf samples, respectively (Figure 2c). The PL spectra were obtained using an excitation wavelength of 430 nm. From these results it can be observed that the addition of solely the LiTf salt (SY+LiTf sample) decreases dramatically the PLQY, when compared to the pristine SY polymer. We ascribe this decrease of PLQY as a result of the quenching of the excitons by the LiTf salt. This is in line with previous reports where it was found that additives, in particular ionic species, can act as interceptors of excitons through the generation of CT non-emissive states and energy transfer processes and thus affect the PLQY.[33–35] However, the addition of Hybrane recovers the PLQY of the sample, as it introduces coordinating sites for the salt. Finally, the SY+Hybrane sample does not show any quenching, as expected. In fact, the PLQY increases slightly compared to the pure SY sample up to 78% due to a slight dilution of the SY which reduces the excitons to migrate and encounter quenching sites. The Hybrane could in this case weaken the close packing of the SY chains and hence decrease the degree of π-interactions.[36]

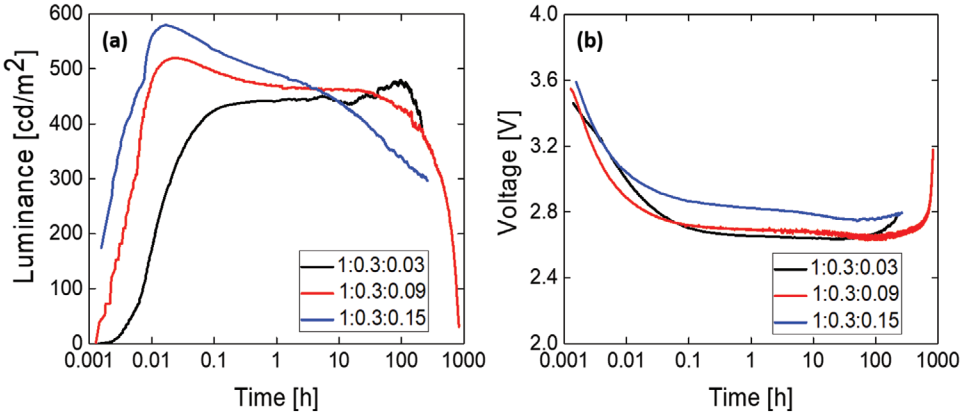

Figure 3. a) Luminance and b) driving voltage of the LECs driven at a constant current density of 75 A m^{-2}. Time is expressed in the log scale.

Devices with three different LiTf concentrations (3%, 9%, and 15%) and fixed Hybrane concentration (30%) were fabricated by sandwiching the SY and Hybrane:LiTf salt blend in between ITO coated glass plates and Al cathodes, and driven with a constant current. A mass ratio of 0.3:0.09 with respect to SY was then selected and driven with a pulsed current bias.

Device luminance and voltage were measured over time under a 75 A m^{-2} constant current density for the different SY:Hybrane:$LiCF_3SO_3$ ratios (**Figure 3**). Over the reported time of 1000 h, it is possible to identify the typical transient states of a LEC. During the turn-on phase the applied voltage decreases. This is the phase where the EDLs are assembling at the interfaces.[37] We notice indeed that in the first instants of operation the voltage decreases as the luminance rises. The starting voltage value for the three devices is around 3.6 V and the turn-on time at 100 cd m^{-2} is faster at higher salt concentrations, with values of 25.2, 7.2, and 3.6 s for 3%, 9%, and 15% of LiTf, respectively. However, a similar effect on the voltage curves is not directly observed as it decreases in the same manner independently from the LiTf amount. In fact, after the EDL is formed, generating an ohmic contact, the remaining ionic species will be used to compensate the charge carries that start to electrochemically dope the CP.

As a result, the luminance keeps increasing and the voltage decreasing until a maximum and a minimum are respectively reached. The maximum luminance values 442, 520, and 580 cd m^{-2} are proportional to the increase of salt content. This could be explained by the fact that, for this system, the amount of LiTf (at least up to 15%) can lead to brighter devices before the doping levels become too severe causing undesired exciton quenching.[38] At the steady-state, the voltage keeps a constant value of around 2.7 V for the 3% and 9% LiTf salt concentration devices and a slightly higher value of 2.9 V for the 15% device. The current efficiency (CE) and PE increase from 5.9 cd A^{-1} and 6.9 lm W^{-1} for 3% of LiTf to 7.7 cd A^{-1} and 8.4 lm W^{-1} for the device with 15% of LiTf content, as the voltage values are rather similar and the luminance increases along the device series. One of the most important features of light-emitting devices is their lifetime. There are several ways to express this, but mostly it is expressed as the time it takes to reach 50% of the initial luminance value, referred to as t_{50}. In OLEDs and inorganic LEDs, the initial luminance is easily adjusted by changing the current density applied. In LECs, however, the initial luminance depends on a number of other parameters and therefore, its lifetime is expressed in more than one manner. Some state the overall luminance that is emitted over its lifetime, this is particularly important for slow starting LECs. Others, use the time it takes to reach a fixed luminance value. In this work, we will report the lifetime using the most commonly used method in LEDs, the time it takes to reach 50% of the initial luminance value. As LECs turn-on relatively fast it allows us to use the maximum luminance as the initial luminance value. Devices with 9% LiTf salt concentration show a measured t_{50} of 530 h whereas the devices that have a LiTf salt concentration of 15% have a reduced lifetime of about 350 h (estimated value). It is not easy to estimate t_{50} for the 1:0.3:0.03 mass ratio but we assume it to be within the interval between 400 and 500 h. We think the so-far best-reported stabilities (t_{50} lifetime) for an SY containing PLEC are 120 h driven by a constant current of 77 A m^{-2}.[22] This is lower than the t_{50} lifetime values we observe under 75 A m^{-2}, namely 530 h (for the 1:0.3:0.09 ratio device). It is worth mentioning that impressive lifetimes over 1000 h and 100 cd m^{-2} were also obtained from SY-LECs prebiased at a constant current density of 77 A m^{-2} and then driven at 19 A m^{-2}.[23,24] It is, however, not straightforward to compare these data directly, as the previously reported devices showed higher maximum luminances and overall increased efficiency. Comparing the lifetime of devices that show different maximum luminances is not a trivial task, as there is a relation between both figures-of-merit and the exact driving conditions might be different. However, these results show that the use of the hyperbranched polymer leads to improvements in the stability of LEC devices. **Table 1** summarizes the principal performances of the above-described devices. Consequently, in order to improve the device performance, we selected the 1:0.3:0.09 ratio as it showed overall better performances when compared to 1:0.3:0.03 and 1:0.3:0.15 ratios.

Devices were prepared with the selected 1:0.3:0.09 active layer ratio and driven under pulsed current biases of 50/75/100 A m^{-2}. The applied pulsed current consisted of block waves at a frequency of 1000 Hz with a duty cycle of 50%. The benefits of a lower current density combined with a pulsed driving current have been demonstrated in previous works and consist in improved stabilities and efficiencies due to the

Table 1. Main performances of LECs under a constant current bias of 75 A m^{-2}.

SY:Hybrane:$LiCF_3SO_3$ ratio	Max Lum. [cd m^{-2}]	t_{50} [h]	Peak CE [cd A^{-1}]	Peak PE [lm W^{-1}]
1:0.3:0.03	442	≈ 400–500	5.9	6.9
1:0.3:0.09	520	530	6.9	7.8
1:0.3:0.15	580	≈ 350	7.7	8.4

presence of "off-states" that limit the growth of the doped zones and side reactions.[39–41] Under pulsed driving conditions the device's performance improves dramatically with respect to the constant current driving (**Figure 4**). Comparing the lifetime data recorded at the same current density it is possible to notice a threefold increase when a pulsed bias is applied. The most important performance parameters of the devices are highlighted in **Table 2**. Peak luminances of 900 and 745 cd m^{-2} are reached with average current densities of 100 and 75 A m^{-2}, respectively. The t_{50} for these rather high initial luminance values are impressive with 850 and about 1000 h. When comparing the luminance over time curves for these higher average current density driven LECs it is clear that from an initially rather flat curve, the decline is increasing exponentially once it starts. This is the result of the combination of the degradation of the devices, as suggested by the dramatic voltage increase (especially in the 100 and 75 Am^{-2} biased devices), and the continuous growth of the doped zones. As a result, the thickness of the intrinsic (non-doped) zone that is responsible for the light generation is reduced which leads to an increased quenching of emitting centers. At the same time, the driving voltage also starts to increase around the inflection point in the luminance time curve which implies that it is increasingly difficult to maintain the set current density. This is most likely the result of permanent degradation. Understanding the degradation of PLECs still remains a challenging task, however, irreversible redox reactions of the CP, as well as changes at the polymer/cathode interface, might be responsible for the progressive decrease of the cell performance.[42,43] At an average current density of 50 A m^{-2} a peak luminance of about 480 cd m^{-2} is reached and these luminance levels are maintained over a long period of time. We have data for devices operated up to 1600 h where the average luminance obtained for the devices is still above 300 cd m^{-2}. An exact t_{50} is not easy to extrapolate since near that point the luminance probably decays superlinear. Nevertheless, we estimate a t_{50} value in excess of 2000 h. This is an order of magnitude higher than what was published previously for similar fluorescent polymer-based LECs.[22–24] Our results are, to the best of our knowledge, one of the most long-lived CP-based LEC in the literature.[9] Moreover, the devices show sub-minutes turn-on times and excellent efficiencies throughout their lifetime. The peak CE and PE obtained for the three devices exceeds 9 cd A^{-1} and 12 lm W^{-1}, with values of 9.6 cd A^{-1} and 12.6 lm W^{-1} for the device biased with a 50 A m^{-2} current density.

To study in depth the effect of the doped zone formation on the stability of our devices, we developed a characterization method that measures the PL of the devices during electroluminescent operation. This is done by modulating the excitation

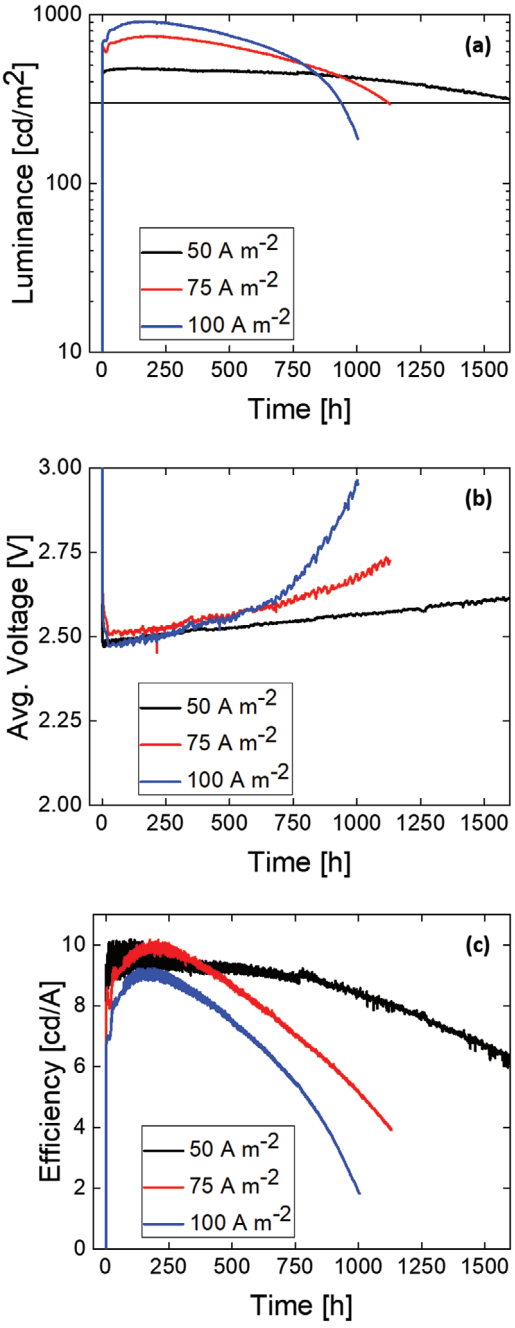

Figure 4. Performance of the 1:0.3:0.09 SY/Hybrane/LiTf ratio devices under an average pulsed current density of 50/75/100 A m^{-2}. a) Luminance, b) Avg. Voltage, and c) CE. Luminance is expressed in the log scale.

Table 2. Main performance parameters of representative LECs under pulsed current average bias of 50/75/100 A m^{-2}.

Average Bias	Max Lum. [cd m^{-2}]	$t_{1/2}$ [h]	Peak CE [cd A^{-1}]	Peak PE [lm W^{-1}]
50 A m^{-2}	480	2000	9.6	12.6
75 A m^{-2}	745	1000	9.9	12.5
100 A m^{-2}	900	850	9.2	12

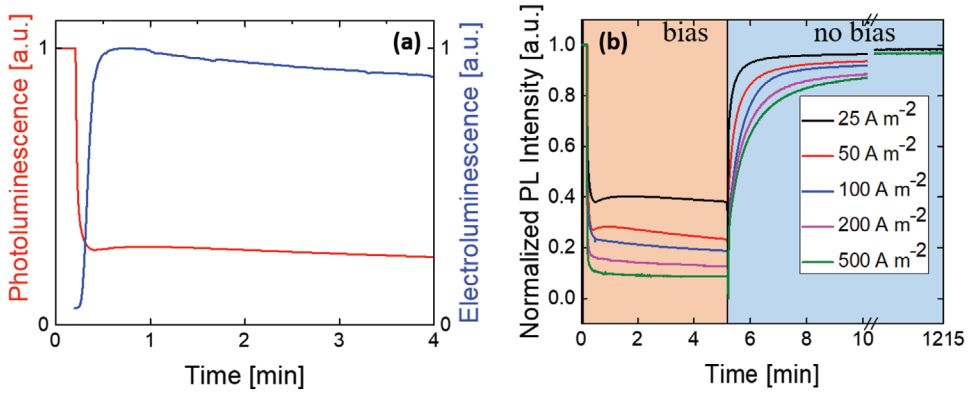

Figure 5. a) PL and EL evolution in the first 4 min of device operation at 50 A m^{-2}. b) Normalized PL intensity, LEC devices biased with a constant current density of 25/50/100/200/500 A m^{-2}. The cells driven at 25 and 500 A m^{-2} were left to recover overnight for about 20 h and measured again. Both measures were taken under a 500 nm light probe.

light source and coupling this modulation to a lock-in amplifier. Hence, the frequency-modulated PL can be detected by the lock-in amplifier in the presence of a non-modulated (constant) EL signal. Using this approach it was possible to extract at the same time the PL and EL profiles and their evolution in the critical first minutes of operation (**Figure 5**).

The intensity of the PL and EL signal followed over time are depicted in Figure 5a. At $t = 0$ the devices are driven at a constant current of 50 A m^{-2}. Prior to turn-on, the PL is stable and the intensity is normalized to this arbitrary value. Upon turning on the bias the PL rapidly decays followed by a more gradual decline. At the same time, the EL slowly rises, typical of the operation of a LEC. In figure 5b, the PL was recorded under different current densities applied to the device (25/50/100/200/500 A m^{-2}), and after the bias was removed. In this graph we omitted to depict the EL for clarity, but it follows the same trend as already depicted in Figure 3. The drop in PL is more pronounced with increasing current density. We attribute this rapid decline in PL to the creation of doped regions that form by the dissociated ions and injected electronic charge carriers. A lower current density, for example, 25 A m^{-2} (black curve), corresponds to a less pronounced quenching when compared to a higher current density, for example, 500 A m^{-2} (green curve). This can be explained by the fact that higher current densities will generate more doping, reducing the intrinsic zone thickness and leaving less doping-free polymer to generate PL. The drop in PL intensity in the LEC is characterized by a first very fast step indicating the rapid ionic movement and doping as well as EDL formation. A second step then follows, 20–25 s after the bias is applied, in which the intensity decays at a slower rate, a possible evidence of the slow growth of the doped zones. As the current is switched off (Figure 5b, blue region "no bias"), two steps can be observed again. The PL first recovers rapidly followed by a slower rate recovery. The speed of PL recovery is proportional to the intensity of the applied bias, as expected. More detailed studies are needed to unravel the exact mechanism, in particular by probing at shorter timescales. However, the fast recovery of the PL signal must imply the removal of the species responsible for its quenching. The quenching of the PL in LECs is generally ascribed to the interaction with the radical cations and anions that form after injecting electrons and holes. Hence, after turning off the bias, these radical cations and anions, rapidly disappear to a large extend. In a timescale of 5 min, the PL signal has recovered to an extent between 96% for the LEC driven under 25 A m^{-2} and 86% for the LEC driven under 500 A m^{-2}. The cells driven at 25 and 500 A m^{-2} were also left to recover overnight for a total time of about 20 h. We can notice that both curves regain PL intensity up to values of 98% and 97%, respectively. As most of the relaxation takes place in the first minutes after the bias for the 25 A m^{-2} current density (black curve) the additional recovery after 20 h is low. On the other hand, for the 500 A m^{-2} current density the relaxation is much slower. There is most likely almost no permanent degradation present in these devices, even at high current biases, as they have been driven for such a short time (5 min). These results might indicate that when the bias is removed the undoping process occurs on different time scales.

The possibility to study the extent of the quenching as well as its decrease over time under bias provides useful insights about LECs doping and undoping mechanisms of different semiconducting materials,[7] ionic transport, and to help assess the origin of undesired side reactions.

3. Conclusion

In conclusion, we introduced a hyperbranched polymer (Hybrane) as the ion dissolving and transporting material in an SY-based state-of-the-art PLEC device. The blending properties of the two polymers have been investigated by means of AFM and PLQY measurements. Our results confirm that SY and Hybrane can form very homogeneous and smooth films without macro-phase separation. Devices were made and were driven under constant and pulsed currents in order to evaluate the stability over time. At low pulsed current densities (50 A m^{-2}), the light-emitting devices showed outstanding lifetimes maintaining a luminance in excess of 300 cd m^{-2} over 1600 operational hours (estimated t_{50} of 2000 h) and excellent current and power efficiencies of 9.6 cd A^{-1} and 12.6 lm W^{-1}, respectively. We measured the PL signal while EL operation of the devices. Our results indicate that the PL signal drops

due to quenching induced by the operation of the LEC. After switching off, the PL is recovered. The transient PL values and degree of recovery are dependent on the current density applied. The ability to monitor both PL/EL in sandwiched LECs will provide new insight into the exact operation and allow for further improvement of the performance.

4. Experimental Section

Materials: All starting materials were obtained from commercial suppliers and used as received. The semiconducting polymer SY has been purchased from Merck, Hybrane DEO750 8500 from Polymer Factory, and $LiCF_3SO_3$ and cyclohexanone from Sigma.

Solution Preparation: Solutions were prepared in an N_2 controlled atmosphere. All the materials were dissolved in separate solutions of cyclohexanone at a concentration of 10 mg mL^{-1} for $LiCF_3SO_3$ and Hybrane, and 12 mg mL^{-1} for SY which was left under continuous stirring and mild heating (50 °C) overnight. Then the precursors were mixed following the mass ratios of 1:0.3:0.03, 1:0.3:0.09, and 1:0.3:0.15 (SY:Hybrane:$LiCF_3SO_3$). These solutions were left under stirring for 1 h. The final SY concentration was 7.5 mg mL^{-1}.

Sample and Device Preparation: Pre-patterned indium tin oxide (ITO)-coated glass plates were used as transparent conductive substrates both for AFM samples and for LEC devices. They were subsequently cleaned ultrasonically in water-soap, water, and 2-propanol baths. After drying, the substrates were placed in a UV-ozone cleaner (Jelight 42–220) for 20 min. The SY solution was then spun at 3000 rpm for 1 min. The as-coated films were annealed for 3 h at 90 °C on a hotplate. A thickness of about 120 nm was obtained for all the three mass ratios. The thickness of the active layer was determined with an Ambios XP-1 profilometer. Finally, an Al electrode (100 nm) was thermally evaporated on top of the active layer using a shadow mask and resulting in multiple active areas of 0.06 cm^2. Similarly, for PLQY measurements the same solutions were spun at 3000 rpm on quartz substrates and annealed for 1 h at 90 °C. The preparation of all the samples, devices, and thermal evaporation was conducted under an N_2 filled atmosphere. Devices were then encapsulated with an Al protecting plate and the Ossila E132 encapsulation epoxy resin. A UV lamp (Hoenle UV Technology, UVACUBE 100) was used to initiate the polymerization reaction of the resin and the samples were left under irradiation for 1 min at a lamp output of 100 W cm^{-1}. The samples were left to rest for another 10 min to make sure that the polymerization reaction reached completion.

Atomic Force Microscopy: AFM measurements were collected in a Multimode atomic force microscope (Veeco instruments, Inc.). The images were obtained with a Si tip with frequency and K of ca. 300 kHz and 40 N m^{-1} respectively using the tapping-mode in air at room temperature. Images were recorded with a 0.5–1 Hz scan rate.

LECs Characterization: The devices were measured by applying a constant current density of 75 A m^{-2} and pulsed current density of 50, 75, and 100 A m^{-2} while monitoring the voltage and luminance versus time by using a True Color Sensor MAZeT (MTCSiCT sensor) with a Botest OLT OLED Lifetime-Test system. The applied pulsed current consisted of block waves at a frequency of 1000 Hz with a duty cycle of 50%. As a result, the average current density and voltage were obtained by multiplying the values by the time-on (0.5 s) and dividing by the total cycle time (1 s). The reported data was the best data observed of at least 3 evaluated cells. There was less than 5 % spreading between these cells.

Photoluminescence Measures: PL spectra and PLQY values were obtained using a Xe lamp and a monochromator as excitation source at 430 nm and an integrated sphere coupled to a spectrometer (Hamamatsu C9920-02 with a Hamamatsu PMA-11 optical detector). All the measurements were conducted under N_2 atmosphere. The PL over time during device operation was measured using a Quartz Tungsten Halogen lamp (Newport model APEX2-QTH) and a monochromator (ORIEL 180) as a tunable excitation source. The excitation wavelength of 500 nm was selected. A silicon photodiode was positioned in close proximity of the device pixel and connected to a lock-in amplifier (Standford Research System SR830 DSP) through a current-voltage converter (Oriel model 71 710) that transforms and amplifies the collected photocurrent into voltage. An optical chopper (New Focus 3502) was connected to the lock-in amplifier and set at a frequency of 327 Hz. The chopper was positioned in front of the light source for the lock-in amplifier to discriminate PL from EL since the former is collected as pulsed light and therefore generates a pulsed photocurrent signal. Finally, the devices were driven at different constant current biases (between 25 and 500 A m^{-2}) using a Keithley 2612A controlled from a personal computer. These measurements were recorded in ambient atmosphere using encapsulated devices.

Acknowledgements

We acknowledge Jorge Ferrando for his help with the PL during EL setup. The research leading to these results has received funding from the European Research Council (ERC) under the European Union's Horizon 2020 research and innovation program Grant agreement No. 834431, the Spanish Ministry of Science, Innovation and Universities (MICIU, RTI2018-095362-A-I00, and EQC2018-004888-P), and the Comunitat Valenciana (IDIFEDER/2020/063 and PROMETEU/2020/077). C.D. acknowledges that the project that gave rise to these results received the support of a fellowship from "la Caixa" Foundation (ID 100010434, code LCF/BQ/DI19/11730020). M.S. acknowledges the MICIU for his RyC contract.

Conflict of Interest

The authors declare no conflict of interest.

Data Availability Statement

Research data are not shared.

Keywords

electroluminescence, hyperbranched polymers, lifetime, light-emitting electrochemical cells, photoluminescence, polymer electrolytes, solid-state lighting

Received: May 5, 2021
Revised: July 12, 2021
Published online:

[1] N. Thejokalyani, S. J. Dhoble, *Renewable Sustainable Energy Rev.* **2014**, *32*, 448.
[2] Q. Pei, Y. Yang, G. Yu, C. Zhang, A. J. Heeger, *J. Am. Chem. Soc.* **1996**, *118*, 3922.
[3] D. L. Smith, *J. Appl. Phys.* **1997**, *81*, 2869.
[4] S. van Reenen, P. Matyba, A. Dzwilewski, R. A. J. Janssen, L. Edman, M. Kemerink, *J. Am. Chem. Soc.* **2010**, *132*, 13776.
[5] M. Lenes, G. Garcia-Belmonte, D. Tordera, A. Pertegás, J. Bisquert, H. J. Bolink, *Adv. Funct. Mater.* **2011**, *21*, 1581.
[6] J. D. Slinker, J. A. DeFranco, M. J. Jaquith, W. R. Silveira, Y. W. Zhong, J. M. Moran-Mirabal, H. G. Craighead, H. D. Abrũa, J. A. Marohn, G. G. Malliaras, *Nat. Mater.* **2007**, *6*, 894.
[7] S. B. Meier, D. Hartmann, D. Tordera, H. J. Bolink, A. Winnacker, W. Sarfert, *Phys. Chem. Chem. Phys.* **2012**, *14*, 10886.
[8] A. J. H. Qibing Pei, G. Yu, C. Zhang, Y. Yang, *Science* **1995**, *269*, 1086.

[9] J. Gao, *ChemPlusChem* **2018**, *83*, 183.
[10] Z. B. Hill, D. B. Rodovsky, J. M. Leger, G. P. Bartholomew, *Chem. Commun.* **2008**, 6594.
[11] W.-C. Chen, C.-S. Lee, Q.-X. Tong, *J. Mater. Chem. C* **2015**, *3*, 10957.
[12] S. Jenatsch, L. Wang, N. Leclaire, E. Hack, R. Steim, S. B. Anantharaman, J. Heier, B. Ruhstaller, L. Penninck, F. Nüesch, R. Hany, *Org. Electron.* **2017**, *48*, 77.
[13] K. Shanmugasundaram, J. C. John, S. Chitumalla, J. Jang, Y. Choe, *Org. Electron.* **2019**, *67*, 141.
[14] J. Choi, S. Kanagaraj, Y. Choe, *J. Mater. Chem. C* **2020**, *8*, 4580.
[15] R. D. Costa, E. OrtÃ, H. J. Bolink, S. Graber, S. Schaffner, M. Neuburger, C. E. Housecroft, E. C. Constable, *Adv. Funct. Mater.* **2009**, *19*, 3456.
[16] A. Pertegás, N. M. Shavaleev, D. Tordera, E. Ortí, M. K. Nazeeruddin, H. J. Bolink, *J. Mater. Chem. C* **2014**, *2*, 1605.
[17] R. D. Costa, E. Ortí, H. J. Bolink, F. Monti, G. Accorsi, N. Armaroli, *Angew. Chem., Int. Ed.* **2012**, *51*, 8178.
[18] H. Xu, R. Chen, Q. Sun, W. Lai, Q. Su, W. Huang, X. Liu, *Chem. Soc. Rev.* **2014**, *43*, 3259.
[19] J. Mindemark, L. Edman, *J. Mater. Chem. C* **2016**, *4*, 420.
[20] S. B. Meier, D. Tordera, A. Pertegás, C. Roldán-Carmona, E. Ortí, H. J. Bolink, *Mater. Today* **2014**, *17*, 217.
[21] C. Poinsignon, *Mater. Sci. Eng. B* **1989**, *3*, 31.
[22] J. Mindemark, S. Tang, H. Li, L. Edman, *Adv. Funct. Mater.* **2018**, *28*, 1801295.
[23] J. Mindemark, S. Tang, J. Wang, N. Kaihovirta, D. Brandell, L. Edman, *Chem. Mater.* **2016**, *28*, 2618.
[24] S. Tang, L. Edman, *J. Phys. Chem. Lett.* **2010**, *1*, 2727.
[25] D. Devaux, R. Bouchet, D. Glé, R. Denoyel, *Solid State Ionics* **2012**, *227*, 119.
[26] K. Timachova, H. Watanabe, N. P. Balsara, *Macromolecules* **2015**, *48*, 7882.
[27] H. Gao, S. Chen, J. Liang, Q. Pei, *ACS Appl. Mater. Interfaces* **2016**, *8*, 32504.
[28] Z. Yu, M. Wang, G. Lei, J. Liu, L. Li, Q. Pei, *J. Phys. Chem. Lett.* **2011**, *2*, 367.
[29] I. Gerz, E. M. Lindh, P. Thordarson, L. Edman, J. Kullgren, J. Mindemark, *ACS Appl. Mater. Interfaces* **2019**, *11*, 40372.
[30] B. Sun, J. Mindemark, E. V. Morozov, L. T. Costa, M. Bergman, P. Johansson, Y. Fang, I. Furó, D. Brandell, *Phys. Chem. Chem. Phys.* **2016**, *18*, 9504.
[31] F. P. Wenzl, P. Pachler, C. Suess, A. Haase, E. J. W. List, P. Poelt, D. Somitsch, P. Knoll, U. Scherf, G. Leising, *Adv. Funct. Mater.* **2004**, *14*, 441.
[32] S. Burns, J. MacLeod, T. T. Do, P. Sonar, S. D. Yambem, *Sci. Rep.* **2017**, *7*, 40805.
[33] J. M. Hodgkiss, G. Tu, S. Albert-Seifried, W. T. S. Huck, R. H. Friend, *J. Am. Chem. Soc.* **2009**, *131*, 8913.
[34] O. V. Mikhnenko, M. Kuik, J. Lin, N. van der Kaap, T.-Q. Nguyen, P. W. M. Blom, *Adv. Mater.* **2014**, *26*, 1912.
[35] S. van Reenen, M. V. Vitorino, S. C. J. Meskers, R. A. J. Janssen, M. Kemerink, *Phys. Rev. B* **2014**, *89*, 205206.
[36] M. A. Summers, S. K. Buratto, L. Edman, *Thin Solid Films* **2007**, *515*, 8412.
[37] S. Tang, L. Edman, *Top. Curr. Chem.* **2016**, *374*, 40.
[38] M. Diethelm, Q. Grossmann, A. Schiller, E. Knapp, S. Jenatsch, M. Kawecki, F. Nüesch, R. Hany, *Adv. Opt. Mater.* **2019**, *7*, 1801278.
[39] D. Tordera, J. Frey, D. Vonlanthen, E. Constable, A. Pertegás, E. Ortí, H. J. Bolink, E. Baranoff, M. K. Nazeeruddin, *Adv. Energy Mater.* **2013**, *3*, 1338.
[40] N. M. Shavaleev, R. Scopelliti, M. Grätzel, M. K. Nazeeruddin, A. Pertegás, C. Roldán-Carmona, D. Tordera, H. J. Bolink, *J. Mater. Chem. C* **2013**, *1*, 2241.
[41] D. Tordera, M. Lenes, H. J. Bolink, *J. Nanosci. Nanotechnol.* **2013**, *13*, 5170.
[42] F. Altal, J. Gao, *Org. Electron.* **2015**, *18*, 1.
[43] J. Fang, P. Matyba, N. D. Robinson, L. Edman, *J. Am. Chem. Soc.* **2008**, *130*, 4562.